Disruption of *BIRC3* associates with fludarabine chemorefractoriness in *TP53* wild-type chronic lymphocytic leukemia

*Davide Rossi,[1] *Marco Fangazio,[1] *Silvia Rasi,[1] Tiziana Vaisitti,[2] Sara Monti,[1] Stefania Cresta,[1] Sabina Chiaretti,[3] Ilaria Del Giudice,[3] Giulia Fabbri,[4] Alessio Bruscaggin,[1] Valeria Spina,[1] Clara Deambrogi,[1] Marilisa Marinelli,[3] Rosella Famà,[1] Mariangela Greco,[1] Giulia Daniele,[5] Francesco Forconi,[6,7] Valter Gattei,[8] Francesco Bertoni,[9,10] Silvia Deaglio,[2] Laura Pasqualucci,[4,11,12] Anna Guarini,[3] Riccardo Dalla-Favera,[4,12,13] †Robin Foà,[3] and †Gianluca Gaidano[1]

[1]Division of Hematology, Department of Translational Medicine, Amedeo Avogadro University of Eastern Piedmont, Novara, Italy; [2]Department of Genetics, Biology and Biochemistry and Human Genetics Foundation, University of Turin, Turin, Italy; [3]Division of Hematology, Department of Cellular Biotechnologies and Hematology, Sapienza University, Rome, Italy; [4]Institute for Cancer Genetics and the Herbert Irving Comprehensive Cancer Center, Columbia University, New York, NY; [5]Hematology Unit, National Cancer Center of Bari and Department of Biology, University of Bari, Bari, Italy; [6]Cancer Sciences Unit, Cancer Research UK Clinical Centre, University of Southampton, Southampton, United Kingdom; [7]Division of Hematology, University of Siena, Siena, Italy; [8]Clinical and Experimental Onco-Hematology, Centro di Riferimento Oncologico Istituto di Ricovero e Cura a Carattere Scientifico, Aviano, Italy; [9]Institute of Oncology Research and [10]Oncology Institute of Southern Switzerland, Bellinzona, Switzerland; [11]Institute of Hematology, University of Perugia, Perugia, Italy; and Departments of [12]Pathology and Cell Biology and [13]Genetics and Development, Columbia University, New York, NY

The genetic lesions identified to date do not fully recapitulate the molecular pathogenesis of chronic lymphocytic leukemia (CLL) and do not entirely explain the development of severe complications such as chemorefractoriness. In the present study, *BIRC3*, a negative regulator of noncanonical NF-κB signaling, was investigated in different CLL clinical phases. *BIRC3* lesions were absent in monoclonal B-cell lymphocytosis (0 of 63) and were rare in CLL at diagnosis (13 of 306, 4%). Conversely, *BIRC3* disruption selectively affected 12 of 49 (24%) fludarabine-refractory CLL cases by inactivating mutations and/or gene deletions that distributed in a mutually exclusive fashion with *TP53* abnormalities. In contrast to fludarabine-refractory CLL, progressive but fludarabine-sensitive patients were consistently devoid of *BIRC3* abnormalities, suggesting that *BIRC3* genetic lesions associate specifically with a chemorefractory phenotype. By actuarial analysis in newly diagnosed CLL (n = 306), *BIRC3* disruption identified patients with a poor outcome similar to that associated with *TP53* abnormalities and exerted a prognostic role that was independent of widely accepted clinical and genetic risk factors. Consistent with the role of *BIRC3* as a negative regulator of NF-κB, biochemical studies revealed the presence of constitutive noncanonical NF-κB activation in fludarabine-refractory CLL patients harboring molecular lesions of *BIRC3*. These data identify *BIRC3* disruption as a recurrent genetic lesion of high-risk CLL devoid of *TP53* abnormalities. (*Blood*. 2012;119(12):2854-2862)

Introduction

The clinical course of chronic lymphocytic leukemia (CLL) ranges from a very indolent disorder with a normal lifespan to a rapidly progressive disease leading to death.[1-3] Occasionally, CLL undergoes histological transformation to Richter syndrome (RS).[4-6] The variable clinical course of CLL is driven, at least in part, by the immunogenetic and molecular heterogeneity of the disease.[7,8]

The genetic lesions identified to date in CLL do not fully recapitulate the molecular pathogenesis of the disease and do not entirely explain the development of severe complications such as chemorefractoriness that still represent a major unmet clinical need.[9-16] In clinical trials, fludarabine refractoriness is due to *TP53* disruption in approximately 40% of CLL patients failing treatment, but in a sizeable fraction of patients, the molecular basis of this aggressive clinical phenotype remains unclear.[17-19] Recently, whole-exome sequencing studies have revealed novel genetic alterations such as *NOTCH1* and *SF3B1* mutations that might potentially contribute to high-risk CLL, although the precise clinical impact of these molecular lesions is still under scrutiny.[20-23]

In CLL, activation of the NF-κB pathway is regarded as a mechanism of resistance to disease eradication.[24-28] Specific interactions between protective microenvironmental niches and CLL cells activate NF-κB signaling, which in turn provides prosurvival signals to the leukemic clone through the up-regulation of several antiapoptotic genes. NF-κB activation is correlated with CLL outcome and enhanced resistance to fludarabine.[25,27,28] In addition to microenvironmental interactions, NF-κB signaling may also be activated in B-cell neoplasia through an array of molecular lesions affecting genes at different levels of the pathway.[29,30] The Baculoviral IAP Repeat Containing 3 (BIRC3) gene, along with TRAF2 and TRAF3, cooperates in the same protein complex that negatively regulates the MAP3K14 serine-threonine kinase, the central activator of noncanonical NF-κB signaling.[31-34]

Submitted November 30, 2011; accepted January 29, 2012. Prepublished online as *Blood* First Edition paper, February 3, 2012; DOI 10.1182/blood-2011-12-395673.

*D.R., M.F., and S.R. contributed equally to this study.

†R.F. and G.G. contributed equally to this study.

The online version of this article contains a data supplement.

The publication costs of this article were defrayed in part by page charge payment. Therefore, and solely to indicate this fact, this article is hereby marked "advertisement" in accordance with 18 USC section 1734.

Table 1. Clinical and genetic characteristics of the consecutive series of newly diagnosed and previously untreated CLL patients

	All (N = 306)		*BIRC3* disrupted (n = 13)		*BIRC3* WT (n = 293)		
	n	%	n	%	n	%	*P*
Age > 65 y	200	65	10	77	190	65	.553
Male	169	55	8	61	161	55	.779
CLL phenotypic score > 3	306	100	13	100	293	100	1.000
Rai stage III-IV	33	11	4	31	29	10	.040
IGHV identity ≥ 98%	98	32	10	77	88	30	.001
TP53 disruption	31	10	0	0	31	11	.376
NOTCH1 mutations	33	11	2	15	31	11	.641
SF3B1 mutations	13	4	2	15	16	5	.173
11q22-q23 deletion	18	6	9	69	9	3	< .001
Trisomy 12	59	19	4	31	55	19	.285
13q14 deletion	160	52	9	69	151	293	.263
Normal FISH	91	30	0	0	91	31	.012

WT indicates wild-type.

After our initial observation of recurrent mutations of *BIRC3* in splenic marginal zone lymphoma,[35] we performed targeted resequencing studies of the *BIRC3* coding sequence and splicing sites across the spectrum of B-cell neoplasia. In the present study, we report that *BIRC3*-disrupting mutations and deletions recurrently and selectively associate with *TP53* wild-type, fludarabine-refractory CLL and predict a dismal clinical outcome in consecutive CLL series.

Methods

Patients

The study population comprised 4 clinical CLL panels representative of different disease phases, including: (1) a consecutive series of newly diagnosed and previously untreated CLL (n = 306; Table 1; median survival from diagnosis, 12.5 years); (2) a cohort of fludarabine-refractory CLL (n = 49; Table 2; median survival from fludarabine-based treatment, 1.8 years); (3) a cohort of fludarabine-sensitive CLL (n = 68; supplemental Table 1 [available on the *Blood* Web site; see the Supplemental Materials link at the top of the online article]; median survival from fludarabine-based treatment, 5.1 years); and (4) a cohort of clonally related RS (n = 33; all diffuse large B-cell lymphomas; supplemental Table 2; median survival from RS transformation, 1.1 year). A consecutive series of clinical monoclonal B-cell lymphocytosis (MBL) with a CLL-like phenotype was also investigated (supplemental Table 3). Diagnosis of MBL, CLL, and fludarabine refractoriness was based on the International Workshop on Chronic Lymphocytic Leukemia-National Cancer Institute criteria.[2] Diagnosis of RS was based on histological criteria.[1]

In addition to CLL, RS, and MBL, we also investigated a cohort of 194 lymphoid tumors representative of the main categories of mature B-cell neoplasms (follicular lymphoma, n = 20; diffuse large B-cell lymphoma.=, n = 30; Burkitt lymphoma, n = 38; extranodal marginal zone lymphoma, n = 65; hairy-cell leukemia, n = 19; and multiple myeloma, n = 22). The number of the mature B-cell neoplasms included in each panel allows a 90% probability of identifying genes that are mutated in at least 10% of patients.

CLL and clinical MBL samples were extracted from fresh or frozen PBMCs isolated by Ficoll-Paque gradient centrifugation. PBMCs were obtained at the following times: (1) for clinical MBL and for the consecutive series of newly diagnosed and previously untreated CLL, at disease presentation; (2) for the fludarabine-refractory CLL cohort, immediately before starting treatment to which the patient failed to respond because of stable/progressive disease; and (3) for the fludarabine-sensitive CLL cohort, at the time of progression immediately before starting the treatment to which the patient responded. All RS studies were performed on RS diagnostic biopsies. Samples of the other lymphoid neoplasms were obtained at diagnosis from the involved site (lymph nodes or extranodal sites in the case of lymphoma; $CD138^+$ cells purified from BM aspirate in

Table 2. Clinical and genetic characteristics of the fludarabine-refractory CLL cohort

	All (N = 49)		*BIRC3* disrupted (n = 12)		*BIRC3* WT (n = 37)		
	N	%	N	%	N	%	*P*
Age > 65 y	36	73	8	67	28	75	.708
Male	31	63	7	58	24	65	.738
CLL phenotypic score > 3	49	100	12	100	37	100	1.000
Rai stage III-IV	28	57	8	67	20	54	.443
Treatment regimen at refractoriness							.499
FCR	17	35	5	42	12	32	
FR	2	4	0	0	2	5	
FC	14	29	2	17	12	32	
F	16	33	5	42	11	30	
IGHV identity ≥ 98%	39	80	10	82	29	78	1.000
TP53 disruption	17	35	0	0	17	37	.004
NOTCH1 mutations	12	24	3	25	9	24	1.000
SF3B1 mutations	12	24	2	17	7	19	1.000
11q22-q23 deletion	13	26	7	53	6	16	.008
Trisomy 12	14	29	3	25	11	30	1.000
13q14 deletion	28	57	7	58	21	57	1.000
Normal FISH	6	12	1	8	5	13	1.000

WT indicates wild-type; FCR, fludarabine, cyclophosphamide, rituximab; FR, fludarabine, rituximab; FC, fludarabine, cyclophosphamide; and F, fludarabine.

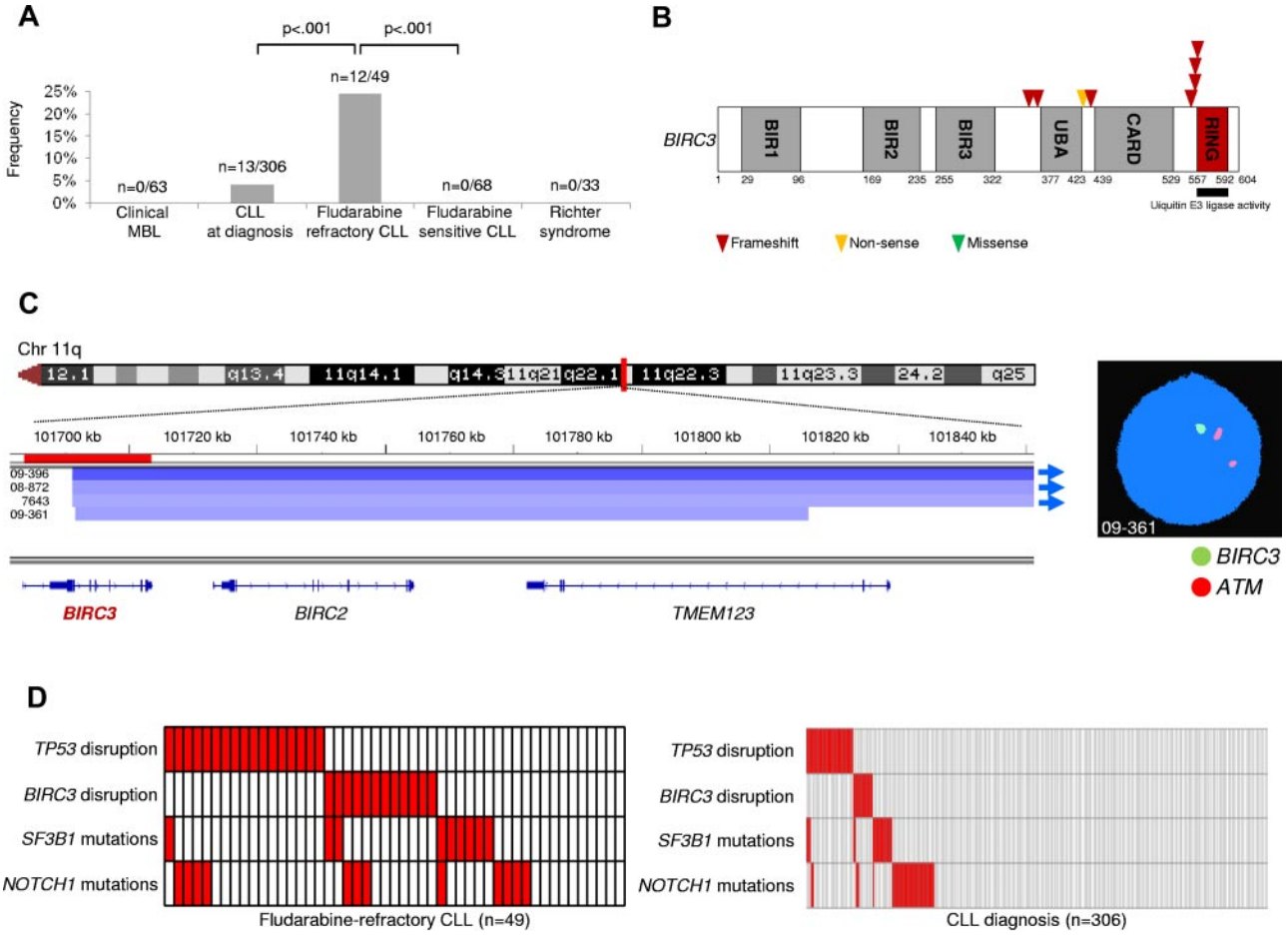

Figure 1. *BIRC3* disruption in CLL. (A) prevalence of *BIRC3* disruption in clinical MBL, in CLL at diagnosis, in fludarabine-refractory CLL, in fludarabine-sensitive CLL, and in RS. Numbers on top indicate the actual number of mutated samples over the total number analyzed. (B) Schematic diagram of the BIRC3 protein with its key functional domains. Color-coded symbols indicate the type and position of the mutations in BIRC3. (C) Graphic representation of segmentation data from 4 CLL patients carrying *BIRC3* deletion. Deletions start from a centromeric break that truncates *BIRC3* and removes its terminal exons, including exon 9, which encodes the RING domain. Sample 09-361 harbors a focal loss of 411 kb on 11q22 involving *BIRC3* and its homolog, *BIRC2*. Each track represents one sample; white denotes a normal (diploid) copy number and blue indicates region of a copy number loss (Integrative Genomics Viewer software; http//www.broadinstitute.org/igv; assembly NCBI36/hg18). Individual genes in the region are aligned in the bottom panel. Dual-color FISH validates the occurrence of 11q22 deletion involving *BIRC3* but sparing *ATM* in sample 09-361 (RP11-177O8-*BIRC3* specific probe in green and LSIATM probe in orange). (D) Mutual relationship of the *BIRC3* disruption with other genetic lesions in CLL at diagnosis and in fludarabine-refractory CLL. In the heat map, rows correspond to identical genes and columns represent individual patients color-coded based on the gene status (white indicates wild-type and red, mutations and/or deletion of *TP53*, mutations and/or deletion of *BIRC3*, mutations of *SF3B1*, and mutations of *NOTCH1*).

the case of multiple myeloma; and peripheral blood purified B cells in the case of hairy-cell leukemia). In all samples, the fraction of tumor cells corresponded to $> 70\%$ as assessed by flow cytometry and/or immunohistochemistry. Matched normal DNAs from the same patients were obtained from saliva or from purified granulocytes and confirmed to be tumor-free by PCR of tumor-specific *IGHV-D-J* rearrangements.[36]

Patients provided informed consent in accordance with local institutional review board requirements and the Declaration of Helsinki. The study was approved by the Ethical Committee of the Ospedale Maggiore della Carità di Novara affiliated with the Amedeo Avogadro University of Eastern Piedmont (protocol code 59/CE; study number CE 8/11).

Mutation analysis of *BIRC3* and *TP53*

The *BIRC3* (exons 2-9, including splicing sites; RefSeq NM_001165.3), *TRAF2* (exons 2-11, including splicing sites; RefSeq NM_021138.3), *TRAF3* (exons 3-12, including splicing sites; RefSeq NM_145725.2), *MAP3K14* (exons 1-17, including splicing sites; RefSeq NM_003954.2), *TP53* (exons 4-8, including splicing sites; RefSeq NM_000546.4), *NOTCH1* (exons 26, 27 and 34; RefSeq NM_017617.2), and *SF3B1* (exons 1-25, including splice sites; RefSeq NM_012433.2) genes were analyzed by PCR amplification and DNA direct sequencing of high-molecular-weight genomic DNA.[11,20,22,23,35] Purified amplicons were subjected to conventional DNA Sanger sequences using the ABI PRISM 3100 Genetic Analyzer (Applied Biosystems). Sequences were compared with the corresponding germline RefSeq sequences using the Mutation Surveyor Version 2.41 software package (SoftGenetics) after both automated and manual curation. All variants were sequenced from both strands on independent PCR products. Synonymous mutations, previously reported polymorphisms (dbSNP135, Ensembl Database, UCSC Genome Browser, or the 1000 Genome Project) and changes present in the matched normal DNA were removed from the analysis. In patients displaying more than one mutational event within the *BIRC3* gene, the allelic distribution of the mutations was determined by cloning and sequencing full-length PCR products obtained from cDNA ($n = 20$ clones). Molecular studies were performed blindly with respect to clinical data. All PCR primers and conditions are available on request.

IGHV mutation status

The Ig heavy variable gene (*IGHV*) mutational status was investigated as described previously.[7] Sequences were aligned to the ImMunoGeneTics sequence directory and considered mutated if identity to the corresponding germline gene was $< 98\%$.[37,38]

Interphase FISH

Probes used for FISH analysis were: LSI13 and LSID13S319 (13q14 deletion), CEP12 (trisomy 12), LSIp53 (17p13/*TP53* deletion), and LSI-ATM (11q2-q23/*ATM* deletion; all from Abbott Laboratories) and the RP11-177O8 (*BIRC3*), RP11-769N4 (*TRAF2*), RP11-676M2 (*TRAF3*), and RP11-666C2 (*MAP3K14*) BAC clones. For each probe, at least 400 interphase cells with well-delineated fluorescent spots were examined. The presence of 13q14 deletion, trisomy 12, 11q22-q23 deletion, 17p13 deletion, *BIRC3* deletion, *TRAF3* deletion, *MAP3K14* gain, and *TRAF2* abnormalities was scored when the percentage of nuclei with the abnormality was above our internal cutoff (5%, 5%, 7%, 10%, 10%, 10%, 10%, and 10%, respectively), defined as the means plus 3 SDs of the frequency of normal control cells exhibiting the abnormality.[6,35]

Copy-number analysis

Copy-number data were derived from a previously reported dataset.[39] Genome-wide DNA profiles were obtained from high-molecular-weight genomic DNA of CLL patients using the Genome-Wide Human SNP Array Version 6.0 (Affymetrix) following the manufacturer's instructions. The bioinformatics pipeline used for the identification of copy-number alterations is described in detail in Rinaldi et al.[39]

Western blot studies

CLL cells were purified by negative selection using anti-CD3, anti-CD14, and anti-CD16 mAbs and Dynal magnetic beads (Invitrogen). Proteins were resolved by SDS-PAGE and analyzed by Western blot. Abs were anti-NFKB2 (#4882; Cell Signaling Technology), anti-BIRC3 (#3130; Cell Signaling Technology), and anti-actin (#sc-1615; Santa Cruz Biotechnology). Image acquisition and densitometric analyses were performed using ImageQuant LAS4000 and TL Version 7.0 software (GE Healthcare). Band intensities were calculated by standardizing over actin and using the JJN3 cell line as an internal loading control in different gels.[35]

Statistical analysis

Overall survival (OS) was measured from date of initial presentation to date of death (event) or last follow-up (censoring).[2] Survival analysis was performed by the Kaplan-Meier method.[40] The crude association between exposure variables and outcome was estimated by univariate Cox regression analysis.[41] The independence of *BIRC3* disruption as a predictor of OS for CLL was estimated after controlling for confounding variables by multivariate Cox regression analysis.[41] The following variables were included in multivariate analysis: *BIRC3* disruption by mutation and/or deletion (present vs absent), age (> 65 years vs ≤ 65 years), Rai stage (III-IV vs 0-II), *IGHV* identity $\geq 98\%$ (present vs absent), 11q22-q23 deletion (present vs absent), *TP53* disruption by mutation and/or deletion (present vs absent), *NOTCH1* mutations (present vs absent), and *SF3B1* mutations (present vs absent). None of the covariates violated the proportional hazard assumption as documented by plotting the smoothed Schoenfeld residuals and by performing a correlation test between time and residuals.[42,43] The assumption of effect additivity of predictors was not violated, as documented by a global test of additivity including interactions between *BIRC3* disruption and other covariates. None of the covariates showed colinearity.[42]

The prediction accuracy of the multivariate survival model was verified by assessing model discrimination and calibration.[42] Discrimination indicates how well the model separates patients who experienced the event of interest from patients who did not, and was measured by calculating the c-index (where 1 is perfect discrimination and 0.5 is equivalent to chance).[42] Calibration describes how well the survival probability from the model corresponds to the survival probability from the observed data and was assessed graphically by plotting the predicted probability of survival against the actual probability of survival.[42] The heuristic shrinkage estimator, which quantifies model overfitting, was calculated using the formula (model likelihood ratio χ^2) − (number of degree of freedom in the model)/(model likelihood ratio χ^2). According to this formula, the more the shrinkage approximates 1, the lower the overfitting of the model.[42] A bootstrap resampling (with 1000 resamples) was used to calculate the bias-corrected c-index and to construct a bias-corrected calibration curve and slope.[42] This approach provides a bias-corrected estimate of prediction accuracy of the model to protect against overfitting.

The stability and predictive performance of *BIRC3* disruption as an independent predictor of OS from CLL was validated internally using a bootstrapping resampling procedure.[42,44] In the first step, 1000 bootstrap samples were generated randomly with replacement from the original CLL population. Cox regression was applied to each bootstrap sample with the same covariates as the original modeling. The percentage of bootstrap samples for which each covariate was selected as significant in the model was then calculated. The percentage of selection reflects the prognostic importance of a covariate, because it is expected that an important covariate will be selected for the majority of bootstrap samples. In the second step, 1000 additional bootstrap samples were generated randomly with replacement from the original CLL population. Cox regression was applied to each bootstrap sample with the same covariates as the original modeling. For each covariate, the mean SD and confidence intervals were computed for the 1000 bootstrap replications.[42,44]

Categorical variables were compared by χ^2 test and Fisher exact test when appropriate. Continuous variables were compared by the Mann-Whitney test. All statistical tests were 2-sided. Statistical significance was defined as $P < .05$. The analysis was performed with the Statistical Package for the Social Sciences (SPSS) Version 18.0 software and with R statistical package Version 2.13.0 (http://www.r-project.org).

Results

BIRC3 mutations across the spectrum of B-cell neoplasia

After the initial observation of recurrent *BIRC3* mutations in splenic marginal zone lymphoma,[35] we performed targeted resequencing of the *BIRC3* coding sequence and splicing sites across the spectrum of B-cell neoplasias. This initial screening revealed that *BIRC3* mutations are selectively restricted to CLL (2 of 20; both cases were primary fludarabine refractory), whereas they are absent in diffuse large B-cell lymphoma (0 of 30), Burkitt lymphoma (0 of 38), follicular lymphoma (0 of 20), extranodal marginal zone lymphoma (0 of 65), hairy-cell leukemia (0 of 19), and multiple myeloma (0 of 22). These results prompted the investigation of the prevalence and clinical impact of *BIRC3* genetic lesions in different clinical phases of CLL.

BIRC3 is frequently targeted by inactivating lesions in fludarabine-refractory CLL

BIRC3 lesions were absent in MBL with a CLL-like phenotype (0 of 63) and were rare in CLL at diagnosis (13 of 306, 4%; n = 3 monoallelic truncating mutations, n = 8 monoallelic deletions, and n = 2 biallelic disruptions by truncating mutation coupling with a deletion; Figure 1A-B and supplemental Tables 3 and 4). Conversely, *BIRC3* was affected in 12 of 49 (24%) fludarabine-refractory CLL patients by inactivating mutations (7 frameshift and 1 nonsense) and/or gene deletions (n = 7; nuclei harboring *BIRC3* deletion: 20%-91%; Figure 1A-B and supplemental Tables 3 and 4). *BIRC3* lesions were similarly represented among patients who received fludarabine-cyclophosphamide-rituximab (FCR) or other fludarabine-based regimens (Table 2). All inactivating mutations were somatically acquired, were predicted to generate aberrant transcripts carrying premature stop codons, and caused elimination or truncation of the C-terminal RING domain, the E3 ubiquitin ligase activity of which is essential for proteasomal degradation of MAP3K14 (Figure 1B).[31-34]

BIRC3 lesions were monoallelic in all but 2 CLL patients (patients 5977 and 6550) who carried inactivation of both *BIRC3* alleles (Table 3 and supplemental Table 4). In patient 5977, a

Table 3. *BIRC3* mutations in CLL

Sample ID	Nucleotide change‡	Amino acid change§	Predicted functional consequence
5977*†	c.1101_1132del32	p.G367fs*6	Truncatedprotein
6550*†	c.1270G > T	p.E424*	Truncatedprotein
6550*†	c.1183_1352del4894	p.V395fs*78	Truncatedprotein
3878*†	c.1279_1280insA	p.I427fs*11	Truncatedprotein
5610*†	c.1638_1639insA	p.Q547fs*12	Truncatedprotein
5889*†	c.1663_1666delAGAA	p.R555fs*12	Truncatedprotein
12632*	c.4388delA	p.E553fs*22	Truncatedprotein
12534*	c.4441_4444delAGAA	p.E553fs*14	Truncatedprotein

*For these patients, paired normal DNA was available and confirmed the somatic origin of the mutation.

†These patients were treated at diagnosis with fludarabine-based regimens to which they failed to respond; therefore, they are included both in the fludarabine-refractory CLL cohort and in the consecutive series of newly diagnosed CLL patients.

‡Numbering according to GenBank accession number NM_001165.3.

§Numbering according to GenBank accession number NP_001156.1.

frameshift mutation of one allele was coupled with a deletion of the second allele. Patient 6550 harbored 3 distinct genetic events on *BIRC3*, including: (1) a monoallelic deletion of the entire *BIRC3* locus in 84% of the nuclei; (2) a large intragenic deletion of 4894 bp that removed the last 142 bp of exon 6, the entire intron 6-7, and the first 285 bp of exon 7 and caused a frameshift mutation (c.1183_1352del, p.V395fs*78) in the gene-coding sequence; and (3) a nonsense truncating mutation (c.1270G > T, p.E424*). In patient 6550, sequencing analysis of *BIRC3* transcripts after cDNA amplification and subcloning demonstrated that the c.1183_1352del intragenic deletion and the c.1270G > T nonsense mutation were located on separate alleles and that the c.1183_1352del intragenic deletion was represented in the majority of the clones, whereas the c.1270G > T nonsense mutation was restricted to 15% of the clones. These data suggest a tumor mosaicism for *BIRC3* in patient 6550.

SNP array analysis of a large CLL dataset (n = 339, including 158 newly diagnosed CLL investigated in this study) identified a focal loss of 411 kb involving *BIRC3* and its homolog *BIRC2* in one CLL (case 09-361; Figure 1C and supplemental Table 4). This deletion truncated *BIRC3* and removed its terminal exons, including exon 9 that encodes the RING domain. Three additional CLL harbored large 11q22 deletions starting from a centromeric break that truncated *BIRC3* and removed its terminal exons, including exon 9 (Figure 1C and supplemental Table 4).

Overall, these data document that *BIRC3* disruption by mutation and/or deletion occurs frequently in fludarabine-refractory CLL, and point to removal of the C-terminal RING domain as a common mechanism altering *BIRC3* function in this context.

Genetic lesions of *BIRC3* cause the formation of truncated BIRC3 proteins and associate with activated NF-κB signaling

Among cases carrying truncating gene mutations, Western blot analysis using Abs directed against the N-terminus of the BIRC3 protein revealed the expression of an aberrant band of lower molecular weight corresponding in size to the predicted truncated BIRC3 (Figure 2). A full-length BIRC3 protein, corresponding to the wild-type allele, was also present. Patient 6550, who carried 3 genetic events, expressed very low levels of both the wild-type and the truncated BIRC3 proteins, with a pattern that is consistent with the occurrence of 2 clonal disrupting deletions and a subclonal truncating mutation in this patient. Patients carrying a monoallelic *BIRC3* deletion displayed reduced levels of BIRC3 protein that were consistent with a residual expression of the wild-type allele (Figure 2).

Western blot analysis of NFKB2 processing from p100 to p52 revealed a constitutive noncanonical NF-κB activation in CLL harboring *BIRC3* disruption by mutations or deletion (Figure 2; mean p52/p100 ratio, 0.565). In contrast, noncanonical NF-κB activation was not observed in patients devoid of *BIRC3* abnormalities, as documented by the predominant expression of p100 over p52 (mean p52/p100 ratio, 0.138) in these patients.

BIRC3-inactivating lesions are specific for fludarabine-refractory CLL and are mutually exclusive with *TP53* disruption

To investigate whether *BIRC3* genetic lesions were restricted to chemorefractory cases in progressive CLL patients, we analyzed *BIRC3* for mutations and deletions in progressive but fludarabine-sensitive CLL and in RS (supplemental Tables 1-3).

Fludarabine-sensitive CLL patients were consistently devoid of *BIRC3* disruption in all cases (n = 68), suggesting that *BIRC3* genetic lesions specifically associate with a chemorefractory phenotype among progressive CLL cases requiring treatment (Figure 1A). *BIRC3* genetic lesions were absent in clonally related RS (0 of 33; Figure 1A and supplemental Table 2), thus strengthening the notion that RS is molecularly distinct from chemorefractory progression without transformation.[6,22]

We then tested the relationship between disruption of *BIRC3* and *TP53* in fludarabine-refractory CLL. In the current series of fludarabine-refractory patients, *TP53* was disrupted by mutations (n = 10) and/or deletions (n = 14) in 17 of 49 (35%) patients. *BIRC3* lesions distributed in a mutually exclusive fashion with *TP53* disruption (Figure 1D). *BIRC3* lesions segregated with *TP53* wild-type, fludarabine-refractory CLL patients (12 of 32, 37%), whereas they were consistently absent among *TP53*-disrupted patients (0 of 17; $P = .004$). These data show that *BIRC3* lesions selectively associate with fludarabine-refractory but *TP53* wild-type CLL across the clinical spectrum of the disease.

By combining *BIRC3* disruption with other genetic lesions enriched in chemorefractory patients (ie, *TP53* disruption, *NOTCH1* mutations, and *SF3B1* mutations), fludarabine-refractory CLL appeared to be characterized by multiple molecular alterations that to some extent are mutually exclusive and account for approximately 80% of cases.

BIRC3 disruption identifies CLL patients whose survival is similar to that associated with *TP53* abnormalities

In a consecutive CLL series evaluated at diagnosis, *BIRC3* disruption (13 of 306, 4%) was associated with unfavorable clinical and genetic features (Table 1) and predicted poor outcome because of primary chemorefractoriness among patients requiring treatment. As shown by univariate analysis, the crude impact of *BIRC3* disruption on survival was an approximately 5-fold increase in the hazard of death (hazard ratio = 5.09; 95% confidence interval,

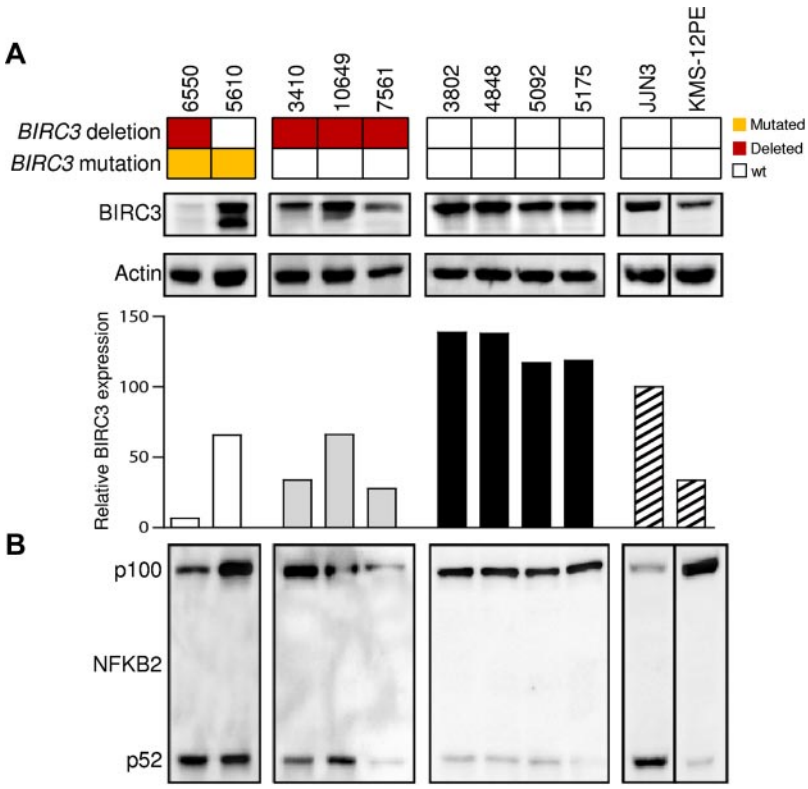

Figure 2. The NF-κB pathway is activated in CLL patients harboring *BIRC3* disruption. Western blot analysis showing BIRC3 expression and NFKB2 processing in purified primary tumor cells from 9 CLL patients carrying wild-type or disrupted *BIRC3*. The JJN3 (plasma cell leukemia) cell line was used as a positive control for NFKB2 processing and BIRC3 expression. The KMS-12PE cell line (a multiple myeloma cell line) was used as a negative control for NFKB2 processing. Actin was used as a loading control. The histogram shows the relative fold change of BIRC3 expression compared with the BIRC3 expression level observed in the JJN3 cell line (arbitrarily set as 100). The aberrant BIRC3 bands in patients 6550 and 5610 correspond in size to the predicted BIRC3-truncated protein.

2.52-10.28; $P < .001$) and a shortening of OS (median OS in *BIRC3*-disrupted patients, 3.1 years vs not reached in *BIRC3* wild-type patients; $P < .001$; Figure 3A and Table 4), which occurred irrespective of the type of *BIRC3* lesion (for mutations, $P = .001$; for deletions, $P = .001$; supplemental Figure 1).

As shown by multivariate analysis, the increased risk of death predicted by *BIRC3* disruption (hazard ratio = 3.04; 95% confidence interval, 1.21-7.61; $P = .017$) was independent of confounding clinical (ie, age and Rai stage) and genetic (ie, *IGHV* mutation status, 11q22-q23 deletion, *TP53* abnormalities, *NOTCH1* mutations, and *SF3B1* mutations) variables at diagnosis (Table 4).

Analogous to CLL analyzed at the time of chemorefractoriness, *BIRC3* disruption and *TP53* abnormalities were also distributed in a mutually exclusive fashion at CLL presentation (mutual information = 0.004; Figure 1D). Because *TP53* abnormalities identify patients with the shortest survival in CLL, the outcome of

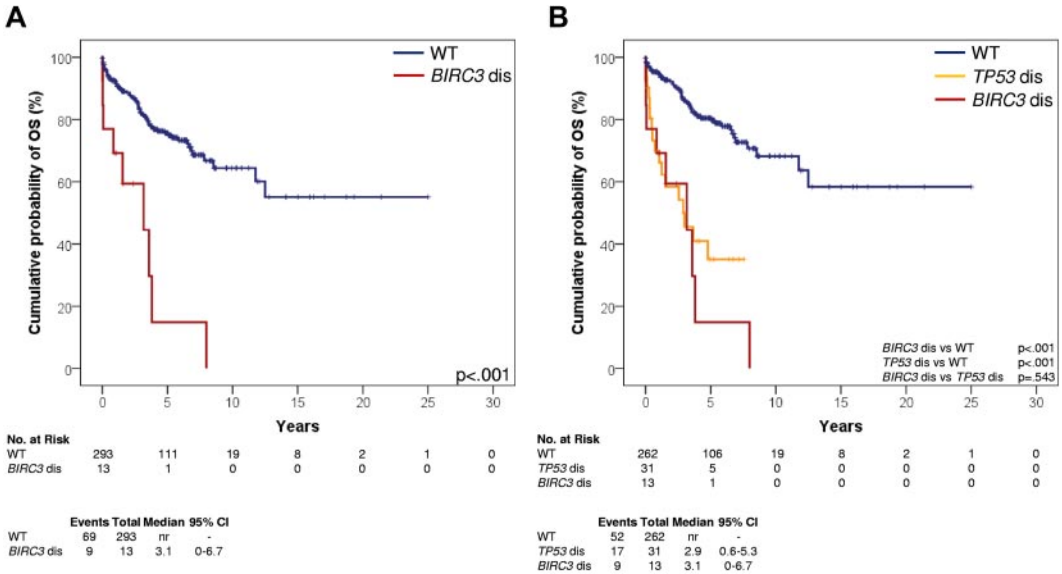

Figure 3. Kaplan-Meier estimates of OS according to *BIRC3* disruption. (A) Kaplan-Meier estimates of OS according to *BIRC3* disruption in newly diagnosed CLL patients (n = 306). *BIRC3* wild-type (WT) patients are represented by the blue line. Patients with *BIRC3* disruption by mutations and/or deletions (*BIRC3* dis) are represented by the red line. (B) Kaplan-Meier estimates of OS according to *BIRC3* and *TP53* disruption in newly diagnosed CLL patients (n = 306). *BIRC3* and *TP53* wild-type patients are represented by the blue line. Patients harboring *BIRC3* disruption but who are wild-type on the *TP53* gene (*BIRC3* dis) are represented by the red line. Patients harboring *TP53* disruption but who are wild-type on the *BIRC3* gene (*TP53* dis) are represented by the yellow line.

Table 4. Univariate and multivariate analysis for OS in newly diagnosed and previously untreated CLL patients

			OS, y			Univariate analysis				Multivariate analysis*†‡				Internal bootstrapping validation			
														Bootstrap parameters, mean			Bootstrap
Characteristic	Events	Total	Median	LCI	UCI	HR	LCI	UCI	*P*	HR	LCI	UCI	*P*	HR	LCI	UCI	selection, %
BIRC3 WT	69	293	NR														
BIRC3 disruption	9	13	3.1	0	6.7	5.09	2.52	10.28	< .001	3.04	1.21	7.61	.017	3.90	1.32	13.17	85%
Age ≤ 65 y	13	106	NR														
Age > 65 y	65	200	8.5	4.6	12.4	3.57	1.95	6.52	< .001	3.88	2.08	7.22	< .001	4.41	2.21	8.87	100%
Rai stage 0-II	56	273	NR														
Rai stage III-IV	22	33	2.7	0.6	4.9	5.44	3.31	8.97	< .001	3.10	1.72	5.59	< .001	3.44	1.83	6.47	97%
IGHV identity < 98%	42	208	NR														
IGHV identity ≥ 98%	36	98	11.7	3.0	20.4	2.03	1.29	3.18	.002	1.24	0.72	2.12	.426	1.31	0.75	2.28	33%
No 11q22-q23 deletion	67	288	NR														
11q22-q23 deletion	11	18	3.1	0.8	5.4	4.08	2.14	7.77	< .001	2.18	0.85	5.62	.105	2.51	0.85	5.64	57%
TP53 WT	61	275	NR														
TP53 disruption	17	31	2.9	0.6	5.3	3.85	2.23	6.65	< .001	4.97	2.75	8.97	< .001	5.30	2.84	9.92	99%
NOTCH1 WT	63	273	NR														
NOTCH1 mutated	15	33	3.3	1.2	14.3	2.15	1.22	3.79	.007	2.08	1.04	4.16	.038	2.31	1.13	4.76	74%
SF3B1 WT	71	288	NR														
SF3B1 mutated	7	18	2.5	1.7	3.3	3.29	1.50	7.21	.003	2.49	1.08	5.72	.032	2.94	1.20	7.35	71%

WT indicates wild-type; HR, hazard ratio; LCI, 95% lower confidence interval; UCI, 95% upper confidence interval; and NR, not reached.
*Shrinkage coefficient, 0.91.
†Discrimination: c-index of the original model, 0.788; bias-corrected c-index, 0.776; optimism, 0.012.
‡Calibration: calibration slope of the original model, 1.000; bias-corrected calibration slope, 0.894; optimism, 0.106.

BIRC3-disrupted cases was compared with that of patients with *TP53* abnormalities. As shown by survival analysis, CLL patients harboring *BIRC3* disruption displayed an OS (median, 3.1 year) similar to that of CLL patients harboring *TP53* abnormalities (median, 2.9 years; $P = .543$; Figure 3B).

BIRC3 is the sole noncanonical NF-κB pathway gene mutated in fludarabine-refractory CLL

To determine the occurrence of genetic lesions of other members of the BIRC3 protein complex,[33] we performed an extensive mutation and FISH analysis of the *TRAF2*, *TRAF3*, and *MAP3K14* genes in fludarabine-refractory CLL patients (n = 49). This analysis did not reveal alterations of *TRAF2*, *TRAF3*, or *MAP3K14*, documenting that *BIRC3* is the sole gene targeted by molecular lesions across all members of the BIRC3 complex.

Discussion

The results of the present study document that *BIRC3* genetic lesions: (1) recurrently and selectively associate with fludarabine-refractory but *TP53* wild-type CLL; (2) at diagnosis, identify patients with a poor outcome similar to that associated with *TP53* abnormalities; (3) exert a prognostic role independent of widely accepted clinical and genetic risk factors; and (4) activate NF-κB signaling.

Fludarabine refractoriness in CLL may be explained by *TP53* disruption in approximately 40% of patients, whereas approximately 60% of high-risk CLL patients are devoid of *TP53* abnormalities.[8,17] This observation prompted the search for other markers of fludarabine refractoriness. Although next-generation sequencing studies have allowed the identification of several previously unrecognized mutated genes in chemorefractory CLL, including *NOTCH1* and *SF3B1*,[20-22] at present, these novel mutations are not numerically sufficient to fully recapitulate the genetics of fludarabine-refractory CLL patients who are wild-type on the *TP53* gene.[20,22]

The candidate gene approach used in this study revealed that genetic lesions of *BIRC3* contribute to clinical aggressiveness and chemorefractoriness in *TP53* wild-type CLL. *BIRC3* disruption selectively occurs in approximately 40% of fludarabine-refractory CLL patients harboring a wild-type *TP53*, whereas it is consistently absent in progressive CLL patients who require treatment but prove to be sensitive to fludarabine-based regimens. At diagnosis, *BIRC3* disruption is rare, but identifies a subgroup of high-risk patients displaying poor survival similar to that associated with *TP53* abnormalities. Confirmation within the frame of prospective clinical trials will be helpful to fully assess the generalization of *BIRC3* disruption as a CLL prognostic marker and as a tool for the early identification of chemorefractory cases.

BIRC3 genetic lesions were absent among clinical MBL cases with a CLL-like phenotype. This observation is consistent with the low frequency in clinical MBL of genetic lesions that are otherwise associated with high-risk CLL, namely *NOTCH1* mutations and *TP53* or *ATM* disruption, and corroborates the notion that clinical MBL is characterized by an indolent biologic phenotype.[45]

BIRC3, along with TRAF2 and TRAF3, cooperates in the same protein complex that negatively regulates MAP3K14, the central activator of noncanonical NF-κB signaling.[31-34] All inactivating mutations of *BIRC3* detected in CLL are predicted to cause the elimination or truncation of the C-terminal RING domain, the E3 ubiquitin ligase activity of which is essential for MAP3K14 proteasomal degradation by BIRC3.[31-34] Consistently, fludarabine-refractory CLL patients harboring *BIRC3* disruption by either mutation and/or deletion display constitutive NF-κB activation.

NF-κB activation is known to provide prosurvival signals to leukemic cells through the up-regulation of several antiapoptotic genes, including members of the BCL-2 family, and to be correlated with both survival and enhanced fludarabine resistance of CLL cells.[24-28] In CLL, NF-κB activation is generally viewed as a consequence of specific interactions between leukemic cells and the microenvironment.[24-28] The present study expands the mechanisms that may sustain NF-κB activation in CLL. In fact, our data suggest that, at least in a fraction of high-risk CLL patients,

leukemic cells might become independent from microenvironmental interactions and may gain active NF-κB signaling through the acquisition of functionally active mutations targeting *BIRC3*. Genome-wide studies have pointed to the potential role of other NF-κB gene alterations, namely mutations of *MYD88*, in CLL development.[20,21] On these bases, the poor prognosis and refractory phenotype associated with *BIRC3* abnormalities might be a consequence of the constitutive NF-κB activation specifically observed among fludarabine-refractory CLL patients harboring *BIRC3* disruption. NF-κB inhibitors are under development in CLL, and preclinical findings suggest that these compounds might be active against chemoresistant CLL clones.[46-49] On these bases, our data might provide a molecular rationale for targeting NF-κB in poor-risk refractory CLL patients.

Identification of *BIRC3* involvement in CLL may be important for elucidating the molecular genetics of 11q22-q23 deletion. In fact, although *ATM* has been regarded as the relevant gene of this chromosomal abnormality,[9,12] biallelic inactivation of *ATM* does not exceed 30% in patients with 11q22-q23 deletion.[13-16] On these bases, a second tumor suppressor in the 11q22-q23 region has been postulated along with *ATM*.[50] *BIRC3*, which maps on 11q22.2 approximately 6 Mb centromeric to the *ATM* gene, might represent an attractive candidate, because: (1) the *BIRC3* locus is included in focal deletions that affect the 11q22.2 band but spare *ATM*; (2) a fraction of 11q22-q23 deletions truncate *BIRC3* and, similarly to *BIRC3*-disrupting mutations, remove its terminal exons encoding the RING domain; (3) analogous to *BIRC3* mutations, *BIRC3* deletions also activate NF-κB signaling; and (4) the poor prognosis marked by *BIRC3* disruption is independent of *ATM* deletion in multivariate analysis.

The identification of *BIRC3* disruption elucidates the molecular basis of a fraction of high-risk CLL cases and expands knowledge of the molecular mechanisms activating NF-κB in this leukemia. In addition to its pathogenetic relevance, *BIRC3* disruption might represent a molecular marker for the early identification of chemorefractoriness among CLL patients who are wild-type on *TP53*, and may provide the rationale for targeted anti–NF-κB therapeutic approaches in this unfavorable clinical setting.

Acknowledgments

This study was supported by the Italian Association for Cancer Research Special Program in Molecular Clinical Oncology (5 × 1000, no. 10007, Milan, Italy, to G.G. and R.F.); Futuro in Ricerca 2008 (to D.R. and S.D.); Programma di ricerca di Rilevante Interesse Nazionale (PRIN) 2008 (to G.G. and R.M.) and PRIN 2009 (to D.R.); Ministero dell'Istruzione, dell'Universitáe della Ricerca, Rome, Italy; Progetto Giovani Ricercatori 2008 (to D.R. and S.D.); Ricerca Sanitaria Finalizzata 2008 (to G.G.); Ministero della Salute, Rome, Italy; Novara–Associazione Italiana contro le Leucemie, linfomi e i mieloma (AIL) Onlus, Novara, Italy (to G.G. and D.R.); Compagnia di San Paolo, Turin, Italy (to R.F.); and the Helmut Horten Foundation and the San Salvatore Foundation (to F.B.). S.M. and S.C. are supported by fellowships from Novara-AIL Onlus, Novara. L.P. is on leave from the University of Perugia Medical School, Perugia, Italy.

Authorship

Contribution: D.R., R. Foà, and G.G. designed the study, interpreted the data, and wrote the manuscript; D.R. and M.F. performed the statistical analysis; M.F., S.R., S. Cresta, A.B., V.S., R. Famà, and M.G. performed the molecular analysis; S.M., C.D., and G.D. performed the FISH analysis; T.V. and S.D. performed and interpreted the biochemical assays; F.B. provided the SNP array data; S. Chiaretti, I.D.G., M.M., and F.F. provided well-characterized biological samples and clinical data; and G.F., V.G., L.P., A.G., and R.D.-F. contributed to data interpretation.

Conflict-of-interest disclosure: The authors declare no competing financial interests.

Correspondence: Davide Rossi, MD, PhD, Division of Hematology, Department of Translational Medicine, Amedeo Avogadro University of Eastern Piedmont, Via Solaroli 17, 28100 Novara, Italy; e-mail: rossidav@med.unipmn.it.

References

1. Müller-Hermelink HK, Montserrat E, Catovsky D, Campo E, Harris NL, Stein H. Chronic lymphocytic leukemia/small lymphocytic lymphoma. Swerdlow S, Campo E, Harris NL, eds; International Agency for Research on Cancer. In: *WHO Classification of Tumours of Haematopoietic and Lymphoid Tissue*. Geneva, Switzerland: World Health Organization; 2008:180-182.
2. Hallek M, Cheson BD, Catovsky D, et al. Guidelines for the diagnosis and treatment of chronic lymphocytic leukemia: a report from the International Workshop on Chronic Lymphocytic Leukemia updating the National Cancer Institute-Working Group 1996 guidelines. *Blood.* 2008; 111(12):5446-5456.
3. Chiorazzi N, Rai KR, Ferrarini M. Chronic lymphocytic leukemia. *N Engl J Med.* 2005;352(8): 804-815.
4. Rossi D, Gaidano G. Richter syndrome: molecular insights and clinical perspectives. *Hematol Oncol.* 2009;27(1):1-10.
5. Rossi D, Spina V, Cerri M, et al. Stereotyped B-cell receptor is an independent risk factor of chronic lymphocytic leukemia transformation to Richter syndrome. *Clin Cancer Res.* 2009;15(13): 4415-4422.
6. Rossi D, Spina V, Deambrogi C, et al. The genetics of Richter syndrome reveals disease heterogeneity and predicts survival after transformation. *Blood.* 2011;117(12):3391-3401.
7. Cramer P, Hallek M. Prognostic factors in chronic lymphocytic leukemia-what do we need to know? *Nat Rev Clin Oncol.* 2011;8(1):38-47.
8. Stilgenbauer S, Zenz T. Understanding and managing ultra high-risk chronic lymphocytic leukemia. *Hematology Am Soc Hematol Educ Program.* 2010;2010:481-488.
9. Döhner H, Stilgenbauer S, Benner A, et al. Genomic aberrations and survival in chronic lymphocytic leukemia. *N Engl J Med.* 2000;343(26): 1910-1916.
10. Zenz T, Kröber A, Scherer K, et al. Monoallelic TP53 inactivation is associated with poor prognosis in chronic lymphocytic leukemia: results from a detailed genetic characterization with long-term follow-up. *Blood.* 2008;112(8):3322-3329.
11. Rossi D, Cerri M, Deambrogi C, et al. The prognostic value of TP53 mutations in chronic lymphocytic leukemia is independent of Del17p13: implications for overall survival and chemorefractoriness. *Clin Cancer Res.* 2009;15(3):995-1004.
12. Stilgenbauer S, Liebisch P, James MR, et al. Molecular cytogenetic delineation of a novel critical genomic region in chromosome bands 11q22.3-923.1 in lymphoproliferative disorders. *Proc Natl Acad Sci U S A.* 1996;93(21):11837-41.
13. Schaffner C, Stilgenbauer S, Rappold GA, Döhner H, Lichter P. Somatic ATM mutations indicate a pathogenic role of ATM in B-cell chronic lymphocytic leukemia. *Blood.* 1999;94(2):748-753.
14. Austen B, Powell JE, Alvi A, et al. Mutations in the ATM gene lead to impaired overall and treatment-free survival that is independent of IGVH mutation status in patients with B-CLL. *Blood.* 2005; 106(9):3175-3182.
15. Guarini A, Marinelli M, Tavolaro S, et al. ATM gene alterations in chronic lymphocytic leukemia patients induce a distinct gene expression profile and predict disease progression. *Haematologica.* 2012;97(1):47-55.
16. Skowronska A, Austen B, Powell JE, et al. ATM germline heterozygosity does not play a role in CLL initiation but influences rapid disease progression through loss of the remaining ATM allele. *Haematologica.* 2012;97(1):142-146.
17. Zenz T, Häbe S, Denzel T, et al. Detailed analysis of p53 pathway defects in fludarabine-refractory chronic lymphocytic leukemia (CLL): dissecting the contribution of 17p deletion, TP53 mutation, p53-p21 dysfunction, and miR34a in a prospective clinical trial. *Blood.* 2009;114(13):2589-2597.

18. Zenz T, Eichhorst B, Busch R, et al. TP53 mutation and survival in chronic lymphocytic leukemia. *J Clin Oncol.* 2010;28(29):4473-4479.
19. Gonzalez D, Martinez P, Wade R, et al. Mutational status of the TP53 gene as a predictor of response and survival in patients with chronic lymphocytic leukemia: results from the LRF CLL4 trial. *J Clin Oncol.* 2011;29(16):2223-2229.
20. Fabbri G, Rasi S, Rossi D, et al. Analysis of the chronic lymphocytic leukemia coding genome: role of NOTCH1 mutational activation. *J Exp Med.* 2011;208(7):1389-1401.
21. Puente XS, Pinyol M, Quesada V, et al. Whole-genome sequencing identifies recurrent mutations in chronic lymphocytic leukaemia. *Nature.* 2011;475(7354):101-105.
22. Rossi D, Bruscaggin A, Spina V, et al. Mutations of the SF3B1 splicing factor in chronic lymphocytic leukemia: association with progression and fludarabine-refractoriness. *Blood.* 2011;118(26):6904-6908.
23. Rossi D, Rasi S, Fabbri G, et al. Mutations of NOTCH1 are an independent predictor of survival in chronic lymphocytic leukemia. *Blood.* 2012;119(2):521-529.
24. Kern C, Cornuel JF, Billard C, et al. Involvement of BAFF and APRIL in the resistance to apoptosis of B-CLL through an autocrine pathway. *Blood.* 2004;103(2):679-688.
25. Endo T, Nishio M, Enzler T, et al. BAFF and APRIL support chronic lymphocytic leukemia B-cell survival through activation of the canonical NF-kappaB pathway. *Blood.* 2007;109(2):703-710.
26. Hewamana S, Alghazal S, Lin TT, et al. The NF-kappaB subunit Rel A is associated with in vitro survival and clinical disease progression in chronic lymphocytic leukemia and represents a promising therapeutic target. *Blood.* 2008;111(9):4681-4689.
27. Buggins AG, Pepper C, Patten PE, et al. Interaction with vascular endothelium enhances survival in primary chronic lymphocytic leukemia cells via NF-kappaB activation and de novo gene transcription. *Cancer Res.* 2010;70(19):7523-7533.
28. Herishanu Y, Pérez-Galán P, Liu D, et al. The lymph node microenvironment promotes B-cell receptor signaling, NF-kappaB activation, and tumor proliferation in chronic lymphocytic leukemia. *Blood.* 2011;117(2):563-574.
29. Compagno M, Lim WK, Grunn A, et al. Mutations of multiple genes cause deregulation of NF-kappaB in diffuse large B-cell lymphoma. *Nature.* 2009;459(7247):717-721.
30. Staudt LM. Oncogenic activation of NF-kappaB. *Cold Spring Harb Perspect Biol.* 2010;2(6):a000109.
31. Vallabhapurapu S, Karin M. Regulation and function of NF-kappaB transcription factors in the immune system. *Annu Rev Immunol.* 2009;27:693-733.
32. Li X, Yang Y, Ashwell JD. TNF-RII and c-IAP1 mediate ubiquitination and degradation of TRAF2. *Nature.* 2002;416(6878):345-347.
33. Zarnegar BJ, Wang Y, Mahoney DJ, et al. Noncanonical NF-kappaB activation requires coordinated assembly of a regulatory complex of the adaptors cIAP1, cIAP2, TRAF2 and TRAF3 and the kinase NIK. *Nat Immunol.* 2008;9(12):1371-1378.
34. Conze DB, Zhao Y, Ashwell JD. Non-canonical NF-κB activation and abnormal B cell accumulation in mice expressing ubiquitin protein ligase-inactive c-IAP2. *PLoS Biol.* 2010;8(10):e1000518.
35. Rossi D, Deaglio S, Dominguez-Sola D, et al. Alteration of BIRC3 and multiple other NF-{kappa}B pathway genes in splenic marginal zone lymphoma. *Blood.* 2011;118(18):4930-4934.
36. Rasi S, Bruscaggin A, Rinaldi A, et al. Saliva is a reliable and practical source of germline DNA for genome-wide studies in chronic lymphocytic leukemia. *Leuk Res.* 2011;35(10):1419-1422.
37. Hamblin TJ, Davis Z, Gardiner A, Oscier DG, Stevenson FK. Unmutated Ig V(H) genes are associated with a more aggressive form of chronic lymphocytic leukemia. *Blood.* 1999;94(6):1848-1854.
38. Damle RN, Wasil T, Fais F, et al. Ig V gene mutation status and CD38 expression as novel prognostic indicators in chronic lymphocytic leukemia. *Blood.* 1999;94(6):1840-1847.
39. Rinaldi A, Mian M, Kwee I, et al. Genome-wide DNA profiling better defines the prognosis of chronic lymphocytic leukaemia. *Br J Haematol.* 2011;154(5):590-599.
40. Kaplan EL, Meier P. Nonparametric estimation from incomplete observations. *Am Stat Assoc.* 1958;53:457-481.
41. Cox DR. Regression models and life tables. *J R Stat Assoc.* 1972;34:187-220.
42. Harrell FE Jr. *Regression Modeling Strategies.* New York, NY: Springer-Verlag; 2001:465-522.
43. Schoenfeld D. Partial residuals for the proportional hazard regression model. *Biometrika.* 1982;69(1):239-241.
44. Chen CH, George SL. The bootstrap and identification of prognostic factors via Cox's proportional hazards regression model. *Stat Med.* 1955;4(1):39-46.
45. Rasi S, Monti S, Spina V, Foa' R, Gaidano G, Rossi D. Analysis of NOTCH1 mutations in monoclonal B cell lymphocytosis. *Haematologica.* 2012;97(1):153-154.
46. Hewamana S, Lin TT, Jenkins C, et al. The novel nuclear factor-kappaB inhibitor LC-1 is equipotent in poor prognostic subsets of chronic lymphocytic leukemia and shows strong synergy with fludarabine. *Clin Cancer Res.* 2008;14(24):8102-8111.
47. Hertlein E, Wagner AJ, Jones J, et al. 17-DMAG targets the nuclear factor-kappaB family of proteins to induce apoptosis in chronic lymphocytic leukemia: clinical implications of HSP90 inhibition. *Blood.* 2010;116(1):45-53.
48. Hertlein E, Byrd JC. Signalling to drug resistance in CLL. *Best Pract Res Clin Haematol.* 2010;23(1):121-131.
49. Herman SE, Gordon AL, Hertlein E, et al. Bruton tyrosine kinase represents a promising therapeutic target for treatment of chronic lymphocytic leukemia and is effectively targeted by PCI-32765. *Blood.* 2011;117(23):6287-6296.
50. Kalla C, Scheuermann MO, Kube I, et al. Analysis of 11q22-q23 deletion target genes in B-cell chronic lymphocytic leukaemia: evidence for a pathogenic role of NPAT, CUL5, and PPP2R1B. *Eur J Cancer.* 2007;43(8):1328-1335.